A R C H I V E S O F M E T A L L U R G Y A N D M A T E R I A L S
Volume 60 2015 Issue 2
DOI: 10.1515/amm-2015-0220

GUANLIN ZHAO*, YONG ZOU*,♯, HUI ZHANG*, ZENGDA ZOU*

EFFECT OF LOW-TEMPERATURE ANNEALING ON THE PROPERTIES OF NI-P AMORPHOUS ALLOYS DEPOSITED VIA ELECTROLESS PLATING

WPŁYW OCENY MIKROSTRUKTURY NA ODPORNOŚĆ KOROZYJNĄ WYŻARZONEGO STOPU AMORFICZNEGO Ni-P

Amorphous Ni-P alloys were prepared via electroless plating and annealing at 200°C at different times to obtain different microstructures. The effects of low-temperature annealing on the properties of amorphous Ni-P alloys were studied. The local atomic structure of the annealed amorphous Ni-P alloys was analyzed by calculating the atomic pair distribution function from their X-ray diffraction patterns. The results indicate that the properties of the annealed amorphous Ni-P alloys are closely related to the order atomic cluster size. However, these annealed Ni-P alloys maintained their amorphous structure at different annealing times. The variation in microhardness is in agreement with the change in cluster size. By contrast, the corrosion resistance of the annealed alloys in 3.5 wt% NaCl solution increases with the decrease in order cluster size.

Keywords: Ni-P amorphous, local atomic structure, corrosion resistance, microhardness

Amorficzne stopy Ni-P otrzymane metodą powlekania bezprądowego wyżarzano w temperaturze 200°C w różnych czasach, w celu otrzymania zróżnicowanej mikrostruktur. Badano wpływ mikrostruktury wyżarzanych stopów amorficznych Ni-P na ich odporność korozyjną w roztworze 3,5% wag. NaCl. Wyniki wskazują, że wielkość klastra w wyżarzanych stopach amorficznych Ni-P najpierw zmniejszyła się, a następnie zwiększyła wraz z czasem wyżarzania. Odporność badanych stopów na korozję jest ściśle związana z wielkością klastra, mimo, że stopy te po wyżarzaniu w różnych czasach zachowują strukturę amorficzną. Odporność wyżarzanych stopów amorficznych Ni-P w roztworze 3,5% wag. NaCl zwiększa się wraz ze zmniejszeniem się klastra.

1. Introduction

Ni-P deposits have attracted considerable attention of numerous researchers because of their unique properties, such as corrosion resistance, wear resistance, paramagnetic characteristics, hardness, and electrocatalytic activity of hydrogen evolution [1-13]. Among these properties, the better corrosion resistance of amorphous Ni-P alloys is investigated widely. The previous results indicated that the corrosion resistance of electroless Ni-P alloys depend upon the chemical composition (P content), substrate structure, preparation of substrate surface, deposit thickness, and subsequent chemical or heat treatment [14].

In generally, Ni-P alloys that contain high phosphorus (>12 wt.%) are considered to be in an amorphous state [15]. However, as to other amorphous alloys, these high phosphorus Ni-P alloys are not fully disordered. In other words, the amorphous matrix includes a specific short-range order or medium-range order cluster. It had been reported that the microstructure affects the properties of amorphous in other amorphous system [16-18]. Bozzini et al. had provided evidence of clustering in amorphous Ni-P prepared via autocatalytic chemical deposition [19], thereby indicating a possibly varied local atomic structure for amorphous Ni-P alloys. The cluster size of Ni-P amorphous alloys not only depends on the phosphorus content or plating technology but is also relative to the heat treatment conditions. When Ni-P alloys is heat treatment in different temperature and times, the size of the cluster should be different. In previous studies [12, 14, 20-22, 23, 24, 25], the effect of crystallizaition on the corrosion of Ni-P alloys have been reported. However, information about the effect of evaluation of microstructure on corrosion resistance of annealed Ni–P amorphous alloys is limited.

This work aims to study the effect of evaluation of microstructure on corrosion resistance of annealed Ni-P amorphous alloys in 3.5wt% NaCl solution As-plated Ni-P samples were heat-treated at 200°C at different durations to obtain annealed samples of amorphous state but with different ordered cluster sizes. The local atomic structure was analyzed via X-ray diffraction. The correlation between properties and local atomic structure was discussed.

2. Experimental procedure

The substrates for electroless plating of Ni-P alloys, which were sized 15 mm×15 mm×3 mm and composed of

* KEY LAB OF LIQUID STRUCTURE AND HEREDITY OF MATERIALS, MINISTRY OF EDUCATION, SHANDONG UNIVERSITY, JINAN 250061, SHANDONG, CHINA
♯ Corresponding author: yzou@sdu.edu.cn

low-carbon steel, were cleaned and polished before plating. In this case, nickel sulfate was used as the nickel source, and sodium hypophosphite was used as the reducing agent. Lactic acid and glycine were used as complexing agents. To determine the effect of local atomic structure on the properties of the Ni-P coating, the samples were subjected to annealing treatment at 200°C at different times. The treatments were conducted using an electric furnace in a controlled Ar atmosphere. The microhardness measurements of annealed Ni-P alloys were carried out under a load of 100g.

The structures of the samples were determined using an X-ray diffractometer with Cu Kα radiation operated at 40 kV/30 mA. The scanning rate and scanning step were fixed at 1°C/min and 0.02°, respectively. The total structure factor S(Q) was calculated using the equation

$$S(Q) = \left[I_{eu}^{coh}(Q) - \sum_i c_i f_i^2 + \left(\sum_i c_i f_i \right)^2 \right] / \left(\sum_i c_i f_i \right)^2 \quad (1)$$

$$Q = \frac{4\pi \sin\theta}{\lambda} \quad (2)$$

where 2θ is the diffraction angle, and λ is the X-ray wavelength. $I_{eu}^{coh}(Q)$ is the coherent X-ray scattering intensity in electron units per atom, which is directly determined from the scattering experiments. f_i and c_i are the atomic scattering factor and concentration, respectively, of the ith element. The pair density function (PDF), G(r), can be obtained through a sine Fourier transform.

$$G(r) = 4\pi r \left[\rho(r) - \rho_0 \right] = \frac{2}{\pi} \int_0^\infty Q[S(Q) - 1] \sin(Qr) dQ \quad (3)$$

where $\rho(r)$ is the atomic density function, and ρ_0 is the average atomic density. The PDF is a measure of the probability of finding an atom at a distance r from another atom [26].

The surface morphology after polarized was observed by a SUPRA^{TM}55 field emission scanning electron microscope (FE-SEM), and the chemical composition of the Ni-P coatings was determined via energy dispersive X-ray spectroscopy (EDS). Anodic potentiodynamic polarization in 3.5wt% NaCl solution was carried out using an AUTOLABP GSTAT302N at a scan rate of 2 mVs^{-1} to investigate the corrosion behaviors of the annealed samples at ambient temperature. A classic three-electrode cell, with the annealed Ni-P sample as the working electrode, a platinum plate (Pt) as the counter electrode, and saturated calomel (SCE) as the reference electrode, was employed for the electrochemical investigations. To prevent the effect of the oxide film, the specimens were polished before being sealed to remove the possible oxide film. The polarization curves were recorded by scanning the electrode potential from -1 V to 1 V. Parameters such as corrosion potential (E_{corr}) and corrosion current density (i_{corr}) were deduced via the Tafel extrapolation method on the recorded data.

3. Results and discussion

As tested by EDS, the phosphorus content was 12.8 wt% of the as-plated Ni-P coating, which belongs to high phosphorus Ni-P alloys. Figure 1 shows the XRD patters of the annealed Ni-P coatings, which were heat-treated at 200°C for 2 h to 48 h. No significant changes in XRD patterns were observed for these samples, and only a single broad amorphous profile was observed. No crystalline peaks were detected, thereby indicating that no crystalline phase was formed at this temperature. However, the shape of the amorphous profiles changed slightly, which indicates that specific microstructural transitions occurred as a result of structural relaxation. The PDFs of these alloys were calculated using Eqs. (1) to (3) to analyze the local atomic structure of these annealed amorphous Ni-P alloys. Figure 2 shows the calculated results of pair distribution functions of annealed Ni-P alloys, which were heat-treated at 200°C for 2, 6, 12, 24, and 48 h. The calculated first coordination radius, correlation radius, and atomic number of the cluster are listed in Table 1. The first coordination radius, which corresponds to the first peak position, was 2.458 Å for all of the samples. Thus, the first coordination radius was unaffected by annealing at 200°C. However, the correlation radius initially decreased and then increased. The correlation radius is generally related to the order cluster size, in which a high order cluster size corresponds to a larger correlation radius. Meanwhile, the atomic cluster number also changed in the same trend, i.e., the cluster number also initially decreased and then increased. This result indicates that the cluster size of amorphous Ni–P alloys decreased during the annealing process when the heat treatment time is less than 12 h. When the heat treatment time exceeded 12 h, the cluster size begins to increase.

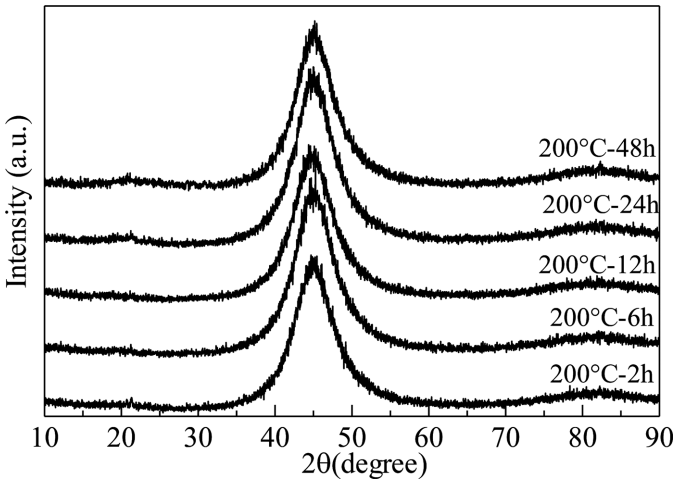

Fig. 1. XRD patterns of the Ni-P alloys annealed at 200°C for different times

TABLE 1
Calculated first coordination radius, correlation radius, and atomic cluster number for Ni-P alloys annealed at 200°C at different times

	200-2h	200-6h	200-12h	200-24h	200-48h
Calculate the first coordination radius	2.458	2.458	2.458	2.458	2.458
Calculate the correlation radius	12.858	11.898	11.738	12.838	13.818
calculate atomic number of cluster	609	482	465	596	785

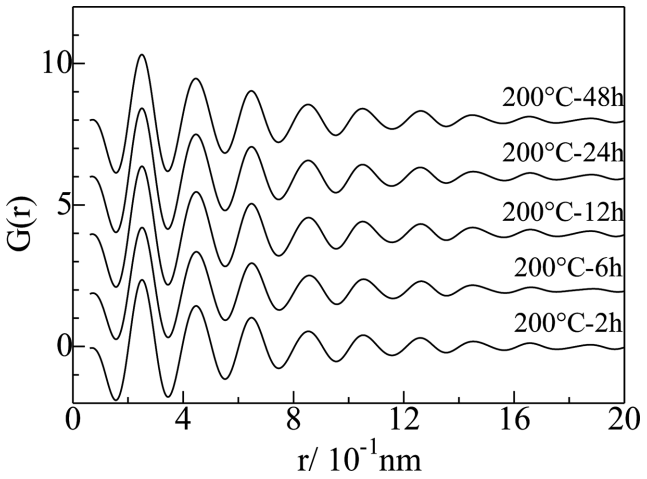

Fig. 2. Pair distribution functions of the Ni-P alloys annealed at 200°C for different times

Figure 3 shows the dependence of the Vickers hardness of the annealed Ni-P alloys on the different annealing durations at 200°C. The microhardness values exhibit the same trend as the correlation radius. That is, the microhardness of the annealed Ni-P alloys initially decreased and then increased. When the annealing time is 12 h, the Ni-P alloys exhibit the lowest hardness. Thus, these annealed samples possess different microstructures, even though they possess similar amorphous structures. The change in microhardness corresponds well with that of cluster size. When the heat treatment exceeded 48 h, the microhardness did not increase further.

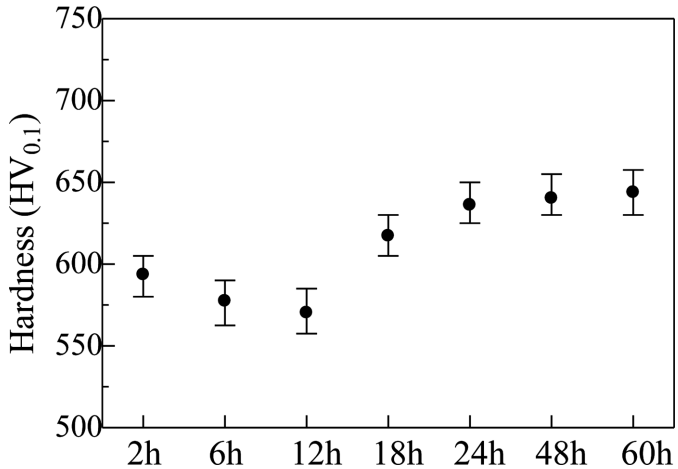

Fig. 3. Variations in Vickers hardness of the amorphous Ni-P alloys annealed at 200°C for different times

Figure 4 shows the respective anodic potentiodynamic polarization curves of the annealed Ni-P deposits in 3.5 wt% NaCl solution. The corrosion potential E_{corr} and corrosion current densityi_{corr} were calculated from the potentiodynamic polarization curves via Tafel extrapolation method. The values of polarization resistance R_p were calculated from the linear polarization curves; the results are summarized in Table 2. The corrosion resistance initially increased and then decreased if corrosion current densityi_{corr} was used to determine the corrosion resistance. The corrosion potential shifted toward the high potential direction, and the corrosion current density decreased with increasing annealing time for the samples that were annealed for less than 12 h. When the annealing times exceeded 12 h, the corrosion potential continued to shift toward the high potential direction, but the corrosion current density increased and polarization resistance decreased. These results indicate that the corrosion resistance begins to decrease at 12 h annealing time. The sample annealed at 200°C for 12 h showed the lowest corrosion rate in 3.5 wt% NaCl solution. As shown in Fig. 4, a broad anode passivation zone is found in the samples annealed at 200°C for 2 h to 12 h. This result indicates that the corrosion mechanism of the amorphous Ni-P alloys can be attributed to protection by a passivation film. For the samples annealed more than 12 h, the anode passivation zone becomes relatively narrow. When the potential is beyond −0.2 V, the corrosion current density shows an evident increase and then decrease, forming anodic peaks, which are marked by an arrow in Fig. 3. This phenomenon corresponds to the collapse of the passivation film.

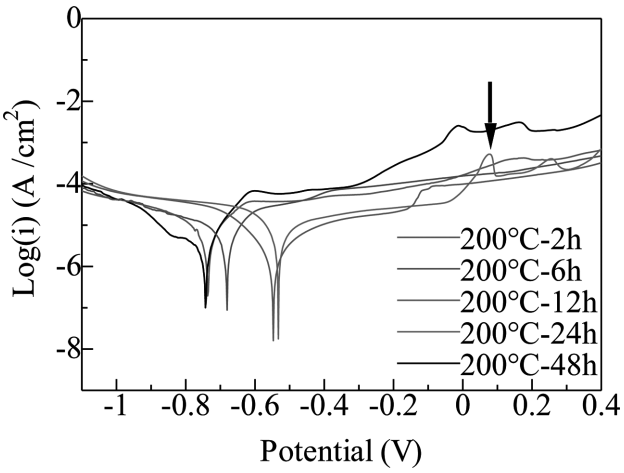

Fig. 4. Polarization curves of the annealed Ni-P alloys annealed at 200°C for different times

TABLE 2
Corrosion parameters obtained from the polarization curves of the annealed Ni-P samples

	I_{corr} (Acm^{-2})	E_{corr}(V)	R_p(.Ωcm^{-2})	Corrosion Rate (mm/a)
2h	4.9942E-5	-0.71844	4221	0.072693
6h	4.7361E-5	-0.6817	4590.2	0.066847
12h	4.0546E-6	-0.54717	8840	0.033897
24h	4.2639E-5	-0.53696	6556.5	0.046799
48h	4.9071E-5	-0.72307	4240.5	0.072359

Figure 5 shows the EIS data acquired in 3.5% NaCl solution for the annealed Ni-P samples as Nyquist plots. Shapes of the Nyquist plots for all the samples were similar, which comprised only one semicircle; the diameters of the semicircles were quite different. The diameter of the Nyquist plot, which determined the corrosion resistance of a material, initially increased and then decreased. The result implied that the corrosion resistance was changed in this order, consistent with that obtained from the polarization test.

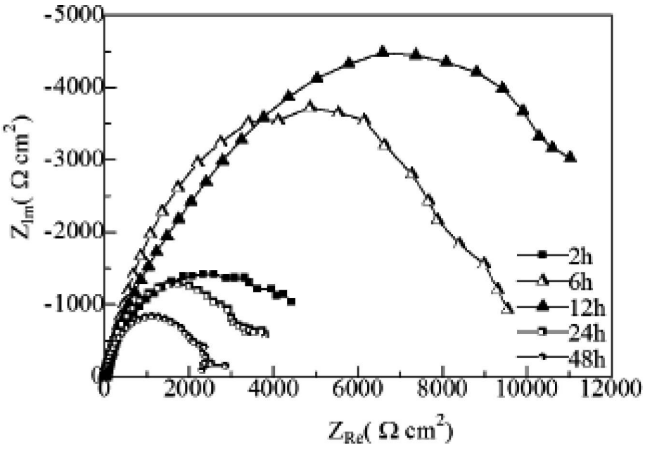

Fig. 5. EIS data acquired in 3.5% NaCl solution for the annealed Ni-P samples as Nyquist plots

Figure 6 shows the SEM image of the annealing 48 h Ni-P alloys after immersing 3.5wt% NaCl solution for 3 weeks. The image shows typical pitting corrosion morphology, which indicates that the annealed Ni-P alloys exhibit microinhomogeneity, which can be attributed to the short-range order clusters. According to the results in Table 1, the cluster size of amorphous Ni-P alloys initially decreased and then increased during the annealing process. The results indicate that microhardness and corrosion resistance are associated with the cluster size.

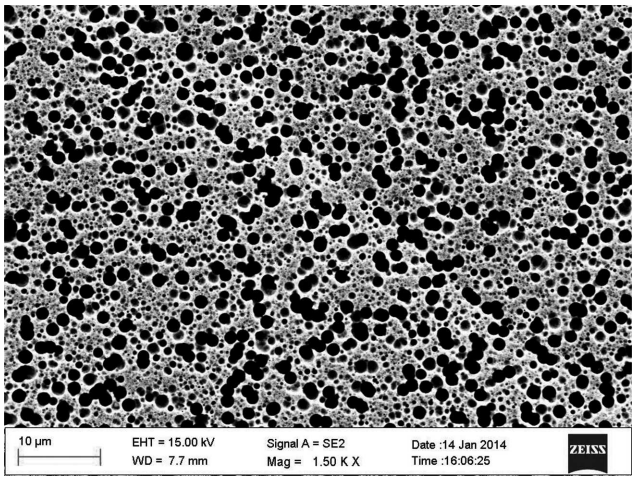

Fig. 6. SEM image of the annealing 48 h Ni-P alloys after immersing 3.5wt% NaCl solution for 3 weeks

The decrease in cluster size of the alloy during the annealing process can initially be attributed to structural relaxation. The as-plated Ni-P coating was subjected to specific vacancy and residual stresses during the electroless process. Certain vacancies may have been filled by nickel or phosphorus atoms via diffusion caused by annealing. Therefore, the homogeneity of the elements was improved, and deposit defects were eliminated through stress relief and porosity agglomeration. As shown in Table 1, the correlation radius that corresponds to the order cluster size gradually decreased when the annealing time is less than 12 h, as well as to the improvement in corrosion resistance. When annealing time is beyond 12 h, the order cluster size began to increase, the corrosion resistance decreased. These phenomena were observed because the atoms in the amorphous Ni-P alloys aggregate in order and form the precursor phase of Ni-P intermetallic compounds, such as Ni_3P, in which the distribution of the elements will not be uniform. A large order cluster size translates to a considerable composition difference between the cluster and matrix. The pitting corrosion morphology presents a good evidence of the microinhomogeneity of the annealed Ni-P alloy. However, the cluster size cannot infinitely increase to form intermetallic compounds. Given that the formation of intermetallic compounds requires active energy, when the annealing temperature is too low to provide the necessary active energy, no crystallization compounds were formed because the annealing temperature (200°C) is far from the crystallization temperature.

The results indicate that the corrosion resistance of amorphous Ni-P alloys is affected by the order atomic cluster size. The increase in the order cluster size increases the composition difference between the cluster and matrix, which negatively affects the corrosion resistance of the amorphous Ni-P alloys by forming significantly more micro-electrochemical cells between the cluster and the matrix. The potentiodynamic polarization testing indicates that anode passivation zone becomes relatively narrow when the annealing time is beyond 12h, which corresponds to the increasing of order cluster.

4. Conclusions

The effects of low-temperature annealing on the properties of amorphous Ni-P alloys were studied. The order cluster size of the Ni-P amorphous alloys affects the microhardness and corrosion resistance. The microhardness initially decreased and then increased with the increase in annealing time, as well as with the increase in the order cluster size. The corrosion resistance in 3.5 wt% NaCl solution shows the opposite trend to the variation of hardness, that is, an initial decrease and then increase are observed. The increase in the order cluster size increases the composition difference between the cluster and the matrix, which negatively affects the corrosion resistance of the amorphous Ni-P alloys by forming more micro-electrochemical cells between the cluster and the matrix. The corrosion morphology of the annealed Ni-P alloys after immersing 3.5wt% NaCl solution for 3 weeks shows the typical pitting corrosion.

Acknowledgements

This project is supported by National Natural Science Foundation of China (No. 51271099).

REFERENCES

[1] R.L. Zeller, III, Corrosion **47**, 692 (1991).
[2] L. Hao, M.-h. Mu, T. Yi, R. Li, Z.-l. Chen, A. Lin, F.-x. Gan, Corros. Sci. Prot. Technol. **20**, 381 (2008).
[3] J. Miskuf, K. Csach, V. Ocelik, E.D. Tabachnikova, V.Z. Bengus, P.S. Popel, V.E. Sidorov, Czech. J. Phys. **54**, D133 (2004).
[4] A. Krolikowski, B. Karbownicka, O. Jaklewicz, Electrochimica Acta **51**, 6120 (2006).
[5] Y. Gao, Z.J. Zheng, M.Q. Zeng, C.P. Luo, M. Zhu, J. Mater. Res. **23**, 1343 (2008).

[6] B. Allen, C. Po-Yao, H. Chi-Chang, Mater. Chem. Phys. **82**, 93 (2003).
[7] C. YanHai, Z. Yong, C. Lin, L. Wen, Mater. Lett. **62**, 4283 (2008).
[8] Y.H. Cheng, Y. Zou, L. Cheng, W. Liu, Mater. Sci. Technol. **24**, 457 (2008).
[9] R. Taheri, I.N.A. Oguocha, S. Yannacopoulos, Mater. Sci. Technol. **17**, 278 (2001).
[10] Y.D. He, H.F. Fu, X.G. Li, W. Gao, Scr. Mater. **58**, 504 (2008).
[11] L.-K. Yang, Y.-F. Jiang, F.-Z. Yang, D.-Y. Wu, Z.-Q. Tian, Surf. Coat. Technol. **235**, 277 (2013).
[12] T. Rabizadeh, S.R. Allahkaram, A. Zarebidaki, Mater. Des. **31**, 3174 (2010).
[13] H.-C. Huang, S.-T. Chung, S.-J. Pan, W.-T. Tsai, C.-S. Lin, Surf. Coat. Technol. **205**, 2097 (2010).
[14] C. Leon, E. Garcia-Ochoa, J. Garcia-Guerra, J. Gonzalez-Sanchez, Surf. Coat. Technol. **205**, 2425 (2010).
[15] M. Crobu, A. Scorciapino, B. Elsener, A. Rossi, Electrochimica Acta **53**, 3364 (2008).
[16] M. Nabiaek, P. Pietrusiewicz, M. Szota, A. Dobrzanska-Danikiewicz, S. Lesz, M. Dospia, K. Boch, K. Ozga, Archives of Metallurgy and Materials **59**, 259 (2014).
[17] P. Pietrusiewicz, M. Nabiaek, M. Szota, M. Dospia, K. Boch, J. Gondro, K. Gruszka, Archives of Metallurgy and Materials **59**, 663 (2014).
[18] S. Pietrzyk, P. Palimaka, W. Gebarowski, Archives of Metallurgy and Materials **59**, 545 (2014).
[19] B. Bozzini, P.L. Cavallotti, Scr. Mater. **36**, 1245 (1997).
[20] Y. Liu, D. Beckett, D. Hawthorne, Appl. Surf. Sci. **257**, 4486 (2011).
[21] J.N. Balaraju, T.S.N.S. Narayanan, S.K. Seshadri, Mater. Res. Bull. **41**, 847 (2006).
[22] H. Ashassi-Sorkhabi, S.H. Rafizadeh, Surf. Coat. Technol. **176**, 318 (2004).
[23] T. Mimani, S.M. Mayanna, Surf. Coat. Technol. **79**, 246 (1996).
[24] Y. Gao, Z.J. Zheng, M. Zhu, C.P. Luo, Mater. Sci. Eng. A, Struct. Mater., Prop. Microstruct. Process. **A381**, 98 (2004).
[25] K.G. Keong, W. Sha, S. Malinov, J. Alloys Compd. **334**, 192 (2002).
[26] M. Saitou, Y. Okudaira, W. Oshikawa, J. Electrochem. Soc. **150**, C140 (2003).

Received: 20 February 2014.